International Journal of Heat and Technology
Vol. 43, No. 6, December, 2025, pp. 2069-2080
Journal homepage: http://iieta.org/journals/ijht

Optimal Heat Transfer of Microchannel Coolers and High Thermal Efficiency Based on Multi-Fin Designs

H.K. Dawood[1], Saad M. Hatem[1*], Saif M. Thabit[2], Yousif Al Mashhadany[3], Ibrahim K. Alabdaly[4]

[1] Department of Mechanical Engineering, College of Engineering, University of Anbar, Ramadi 31001, Iraq
[2] Directorate of the Highest Euphrates, General Company of Electrical Energy Distribution / Middle Region, Ministry of Electricity, Haditha 31004, Iraq
[3] Biomedical Engineering Research Center, University of Anbar, Ramadi 31001, Iraq
[4] Department of Chemical and Petrochemical Engineering, College of Engineering, University of Anbar, Ramadi 31001, Iraq

Corresponding Author Email: saad.mottlag@uoanbar.edu.iq

https://doi.org/10.18280/ijht.430607

Received: 11 July 2025
Revised: 16 October 2025
Accepted: 29 October 2025
Available online: 31 December 2025

Keywords:
optimal heat transfer, microchannel coolers, thermal efficiency, multi-fin designs

ABSTRACT

In this work, the effects of three different fin shapes on thermal and fluid flow characteristics for flowing water at Reynolds numbers that vary between 100 and 500 are examined within a miniature channel heat sink (MCHS). The consequences of these fin configurations (Cases A, B, and C) were compared to an analogous case absent fins (Case S) using the finite volume approach, which was implemented using ANSYS software. Important variables were assessed, such as the hydrothermal performance factor, ordinary wall temperature, mean Nusselt number, and friction factor. Findings showed that adding fins significantly increased heat transfer rates: at Re = 500, Case C had a 66% improvement, preceding Cases A (36%) & B (31%). In every example, the average Nusselt coefficient rose as Reynolds numbers rose, yet the average wall temperature and friction factor fell as Reynolds numbers rose. Interestingly, Case C had the highest efficiency with the best thermal coefficient of performance of almost 1.3 at Re = 500. These results highlight how important fin design is to improving microchannel coolers' thermal performance and advancing the creation of more effective cooling systems.

1. INTRODUCTION

Due to modern digital devices having increasing power density and compactness, it is difficult to build efficacious and small cooling elements for larger heat-generating processors. These devices' principal function is to keep electronic modules within the design's designated temperature range. Microchannel heat sinks seem to be perfect for this goal since they are compact and efficient, unlike conventional MCHS, which need a large surface area to greatly increase heat transfer enhancement rates significantly [1]. Semiconductor devices are commonly employed in many different applications, including solar cells, CPU components, and microelectronics. It has been noted that these devices' performance is very susceptible to operating temperature [2, 3]. Therefore, as chips achieve larger power densities, thermal management techniques become increasingly crucial [4].

The foundation of a microchannel heat sink is the use of liquid-cooling tubes with a small diameter. The heat transfer rate is improved by these narrow passages because they offer a significant surface area for heat transfer between the coolant and the chip. However, there are significant design limitations when using microchannel heat sinks to cool small electronic devices. To effectively dissipate heat generated at a given rate, the temperature increase, pressure drop, and coolant flow rate must be adjusted in the microchannel heat sink [5]. Zeng et al. [6] demonstrated flow and heat performance in a microchannel. Zhu et al. [7] investigated the increase of heat transfer in microchannels with grooved side surfaces. Zhu et al. [8] presented the performance factor of heat transfer and fluid flow in microchannels with fan-shaped cavities. Copeland et al. [9] simulated thermal and fluid flow fields using a 3D flow of microchannels.

Microelectronic refrigeration, heat exchangers, combustion chambers, aeroplanes, and medical and biological equipment are among the many uses for undersized thermal systems that have lately emerged in applied science and technology. In such circumstances, the usage of microsystems has become more common, and numerous engineering and scientific investigations have been performed to develop more enhancement technologies [10]. From an applied standpoint, energy assessments and heat transfer analysis are critical in the innovative design of microsystems. Liao and Zhao [11] demonstrated energy transfer via a small tube utilizing supercritical carbon dioxide. The efficiency of nanofluid in a tiny heat sink was discovered by Ashjaee et al. [12].

Many researchers [13-22] performed various microchannel heat sinks numerically with different geometric designs of flow fields and heat transfer. Their findings suggest that the changes in the geometric design of the discharge field channels can increase the heat transfer coefficients, but at the expense of increased pressure drop and friction factor compared to the

standard smooth microchannel. As a result of their high thermal conductivity have been proposed to be used as super-coolants in microchannel heat sinks to improve heat removal [23, 24]. However, it is well understood that the coefficient of heat transfer *(h)*, which is a definition of heat transfer efficacy, is directly proportionate to specific heat capacity *(Cp)*, density *(ρ)*, and thermal conductivity *(k)*, and inversely proportionate to surface tension *(σ)* and viscosity *(μ)* if a phase change is applied [25]. Although dispersing nanoparticles in base fluids increases density and thermal conductivity. As a result, a thorough analysis is required to determine the benefits and drawbacks of employing nanofluids in MCHS [25-27].

Utilising the quick and ongoing advancements in computers and computing methods, computational fluid dynamics (CFD) approaches are powerful tools for modelling fluid flow and the related heat and mass transport by numerically solving the mathematical equations that govern these processes. The results of CFD simulations may be applied to the following fields: in-depth product research and development; conceptual studies of new and redesigned designs; troubleshooting; and thorough, detailed analysis [28]. When compared to analytical and experimental fluid dynamics, CFD can offer comprehensive information, visualisation, and a detailed investigation, which makes it crucial for simulations of micro-electro-mechanical-systems (MEMS) applications, especially in the design of effective microchannel heat sinks. And CFD may solve a variety of challenging issues that are beyond the reach of analytical approaches [29, 30]. As a result, CFD enhances fundamental understanding of fluid flow, mass, and heat transfer properties, which are critical in the design and process management of microchannel heat sinks.

Many studies have been conducted over the last few decades to investigate the behaviour of thermal and flow characteristics in different types of MCHS. Qu and Mudawar [31] investigated heat transport properties in a rectangular MCHS cooled by pure water. The temperature rose about linearly along the primary flow path in both the fluid and solid areas. Moreover, the maximum temperature was found at the base wall of the heat sink, directly above the channel's outflow. Xie et al. [32, 33] investigated the laminar and turbulent flow and heat transfer properties of a water-cooled directly MCHS numerically. Heat fluxes ranging from (256 to 350 W/cm^2) were reduced for a closely-optimized microchannel, while pumping power rose from (0.205 to 5.365 W). Using statistical methods, Sui et al. [34] examined heat and liquid flow in 3D wavy MCHS with rectangular cross-sections. The simulation results showed that the wavy microchannel outperformed the straight rectangular channels with identical cross-sections in terms of thermal performance. Moreover, the enhancement in heat transfer may be far greater than the penalty for pressure losses. Laminar flow and thermal in longitudinal and transversal wavy MCHS for electronic chip cooling were recently studied by Xie et al. [35, 36]. The outcomes displayed that the transversal wavy microchannel overreached the conventional straight MCHS in terms of overall heat transfer enhancement, particularly at higher wave amplitudes at the same Reynolds number.

The microchannel heat sinks were constructed using similar theory-based methods. For instance, Zhang et al. [37, 38] used experimental and computational studies to examine the heat transfer characteristics of multiple microchannel heat sinks in single-phase liquid flow under various heat flux and flow rate conditions. Although it had a greater maximum temperature, the heat sink with U-shaped channels distributed the temperature more evenly than the serpentine channels. The flow and heat fields of asymmetric/symmetric leaf-like and tree-like branching networks employed in electronic cooling were simulated by Wang et al. [39, 40]. They found that the maximum inlet-to-outlet fluid temperature differential and pressure drop may be considerably decreased by offset in leaf-like branching networks. Gilmore et al. [41] thoroughly examined and evaluated several studies that considered concentrator photovoltaic active cooling techniques. They concluded that a workable option for high-density heat fluxes is single-phase microchannel cooling. The most current experimental and numerical studies on MCHS geometric designs for heightened heat flux applications were compiled by Naqiuddin et al. [42]. According to the review, one crucial factor that significantly affects the flow heat transfer process is the geometric design of microchannels.

A microchannel cooling device with a complex design was analytically examined by Di Capua et al. [43] at high heat flux levels. The findings indicated that a microchannel device could maintain a chip temperature below 28°C. With inclined fins, a unique small heat sink was optimised for heightened heat flux applications by Alfellag et al. [44]. The fluid flow and heat transfer enhancement of the investigated heat sink improved when the tendency angle of the slots was widened up to 55°C. Ali et al. [45] presented a numerical analysis to investigate the effect of V-shaped attack rib angle on the hydrothermal performance of MCHC over a Reynolds number range of Re = 100 - 900. The results indicated that a rib angle has a significant influence on the thermal and flow field. Okab et al. [46] investigated the thermal efficiency of microchannels with sidewall dimples (1 mm and 0.5 mm) and a fillet shape on the lower surface under a laminar range (Re = 200 - 1200). Outcomes showed that dimples and the fillet profile particularly enhance thermal performance. Attached, these characteristics achieved a 60% higher Nu compared to straight microchannels. In fan-shaped cavity microchannels, Ali et al. [47] investigated seven distinct rib placements and found that the front and rear configurations significantly enhance flow mixing, leading to a 19% increase in the Nu in comparison to standard designs. Li and Chen [48] investigated a double-layered MCHS that used both solid and porous ribs in combination with microencapsulated phase change materials, in contrast to traditional solid rib designs, resulting in a significant improvement in the heat transfer. Additionally, Li et al. [49] described a microchannel heat sink with a slant rib-quatrefoil rib arrangement that greatly improved heat transfer performance, leading to a 131% increase in the Nu and a 66.6% drop in thermal resistance at Re = 696.

Microchannel heat sinks (MCHS) have been the subject of extensive research into developing innovative fin designs to enhance their hydraulic and thermal performance. Porous fins have been the subject of some studies that sought to improve heat transfer, while microinserts have been the subject of other studies that sought to alter fluid flow and heat transmission. However, there are still a lot of unanswered questions about how different MCHS fin configurations impact important parameters across a range of Reynolds numbers (100 to 500), including the average Nusselt number, friction factor, mean wall temperature, and hydrothermal performance factor.

Our work is unique since it examines three different fin designs in an MCHS and does it over a wide range of Reynolds numbers. We compare the thermal and hydraulic performance of these suggested designs to a baseline situation without fins using the finite volume approach and numerical simulations in

ANSYS software. This method provides new information about how to optimize fin layouts for better thermal performance. This research gap can be filled by our study contributes to the advancement of microelectronics cooling technology by offering comprehensive insights on fin design optimization, especially for applications that demand efficient heat dissipation in small places.

A summary of the comparative analysis of the hydrodynamic and thermal performance of micro-heatsinks with various fin designs is provided in Table 1.

Table 1. Comparative evaluation of microchannel heat sinks' thermal and hydrodynamic performance with various fin configurations

Ref. No.	Publish Year	Technology Applied	Average Heat Transfer	Thermal Efficiency
[1]	2020	Nanofluid-based microchannel heat sink	Improved due to nanofluid enhancement	High thermal performance reported
[5]	2016	Micro heat sink for power transistor using CFD	Moderate	Limited efficiency due to design simplicity
[6]	2021	Open-ring pin fins in microchannels	Significant improvement	Enhanced due to turbulence
[7]	2021	Grooved microchannels	Increased Nusselt number	High thermal efficiency
[8]	2021	Fan-shaped cavities with rib configurations	Enhanced mixing	Balanced efficiency with moderate losses
[9]	1997	Manifold microchannel heat sinks	Uniform heat distribution	Isothermal efficiency
[10]	2023	Hybrid nanofluid-based microchannel heat sink	High heat transfer rates	Superior cooling performance
[11]	2002	Supercritical CO2 flow	Moderate	Low thermal resistance
[12]	2015	Magnetic nanofluids in heat sinks	Enhanced forced convection	Improved under magnetic field
[13]	2013	Periodic expansion-constriction cross-sections	Increased heat transfer coefficients	High efficiency
[14]	2013	Bifurcation microchannels	Improved laminar flow	Efficient heat dissipation
[15]	2014	Multiple-length bifurcation microchannels	Enhanced thermal gradients	High thermal-hydraulic performance
[16]	2016	Fan-shaped ribs on sidewalls	Reduced pressure drop	Balanced performance
[17]	2016	Fan-shaped ribs (pressure drop analysis)	Consistent heat transfer	Moderate
[18]	2016	Fan-shaped ribs (thermal characteristics)	Improved heat transfer	High
[19]	2017	Wavy porous fins	Simultaneous reduction in pressure drop	High thermal efficiency
[20]	2018	Slant rectangular ribs	Parameter-dependent heat transfer	Variable
[21]	2018	Internal vertical bifurcations	Enhanced laminar flow	High efficiency
[22]	2018	Dimple and pin fin configurations	Optimized flow and heat transfer	High thermal performance
[23]	1999	Nanoparticle-enhanced fluids	Increased thermal conductivity	High
[24]	1995	Nanofluids	Enhanced thermal properties	High
[25]	2009	Review of nanofluids	Mixed results	Application-specific
[26]	2009	Benchmark study on nanofluids	Variable heat transfer	Moderate
[27]	2020	Hydrothermal behavior in a curved annular tube	Enhanced mixing	High efficiency
[28]	2010	PEM fuel cell transport phenomena	Not applicable	High electrochemical efficiency
[29]	2009	Hygro-thermal stresses in PEM fuel cells	Not applicable	High durability
[30]	2009	Deformation prediction in PEM fuel cells	Not applicable	High reliability
[31]	2002	Single-phase microchannel heat sink	High heat transfer rate	High efficiency
[32]	2007	Turbulent heat transfer in minichannels	Enhanced turbulent mixing	High thermal performance
[33]	2009	Laminar heat transfer in minichannels	Improved heat transfer coefficients	High efficiency

2. THEORETICAL MODEL AND NUMERICAL PROCEDURE

2.1 Physical model

In the actual application, the straight channel heat sink has 120 parallel microchannels with a rectangular cross-sectional area with a height of channel H = 0.4 mm and a bottom size of (L × W) 30 × 30 mm^2. However, to reduce the simulation time and size of the grid due to the symmetry condition, a single-branch microchannel is taken as the computational model, as shown in Figure 1(a). The straight microchannel heat sink (MCHS-S) is utilized as the baseline microchannel heat sink to estimate the enhancement by the different rectangular fins in microchannel heat sinks in terms of hydro-thermal performance and fluid flow behavior. There are three cases of microchannel heat sink as shown in Figure 1(b), The MCHS-A is a microchannel heat sink with two rectangular fins in the bottom wall of the middle of microchannel, The MCHS-B is a microchannel heat sink with four rectangular fins in the bottom wall, two in the inlet of channel and two in the outlet of channel, while the MCHS-C including five rectangular fins, one in the top wall of channel and four in the bottom of inlet and outlet of channel. Figure 2 illustrates schematically the

cases studied in this work, and the detailed geometric parameters are summarized in Table 2.

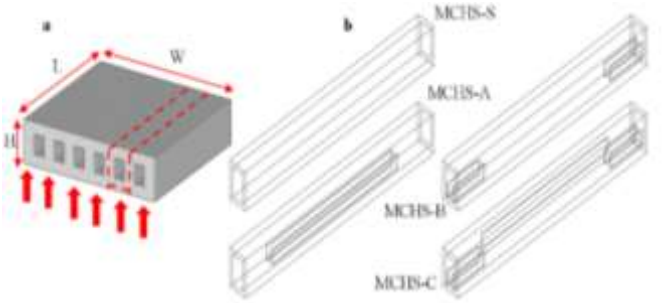

Figure 1. Schematic diagram of MCHS: (a) Integrated model of MCHS; (b) Isometric view of MCHS with different fin configurations

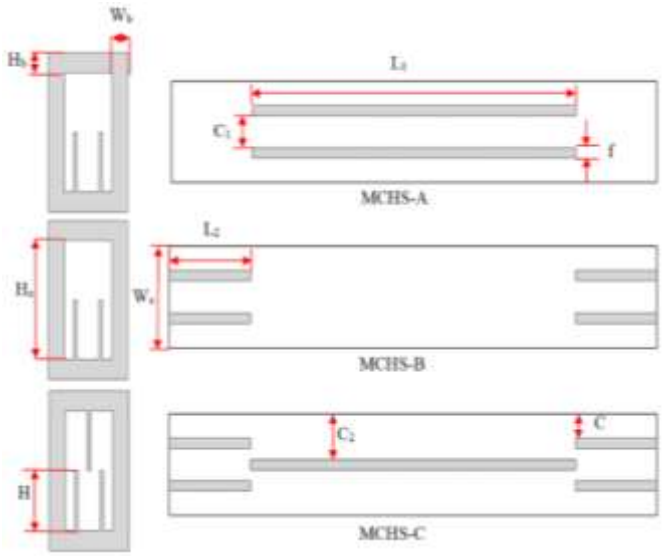

Figure 2. Schematic diagram of different microchannels with fins

Table 2. The size parameters utilized in the current study

Geometric Parameters	Value (μm)	Geometric Parameters	Value (μm)
H	400	**H_c**	300
W	30,000	**H_b**	50
L	30,000	**H_f**	150
L_1	20,000	**C_1**	70
L_2	5000	**C_2**	70
W_c	150	**C_3**	30
W_b	50	**f**	10

2.2 Mathematical model and boundary conditions

A mathematical model of fluid flow and thermal performance processes in the micro-channel heat sink is established in this study based on the following assumptions:

1. The flow is laminar, incompressible, single phase, and steady state.
2. There is a no-slip boundary condition between the fluid and the walls.
3. The radiation heat transfer, gravitational force, and surface tension are not considered.

Based on the above assumptions, the steady-state conservation for momentum, mass, and energy equations in the fluid are defined as [50, 51]:

The Continuity equation:

$$\frac{\partial u}{\partial x}+\frac{\partial v}{\partial y}+\frac{\partial w}{\partial z}=0 \tag{1}$$

where, u, v, w in m/sec are the velocity in x, y, z direction respectively.

The Momentum equations:

$$u\frac{\partial u}{\partial x}+v\frac{\partial u}{\partial y}+w\frac{\partial u}{\partial z}=-\frac{1}{\rho}\frac{\partial p}{\partial x}+\frac{\mu}{\rho}\left(\frac{\partial^2 u}{\partial x^2}+\frac{\partial^2 u}{\partial y^2}+\frac{\partial^2 u}{\partial z^2}\right) \tag{2}$$

$$u\frac{\partial v}{\partial x}+v\frac{\partial v}{\partial y}+w\frac{\partial v}{\partial z}=-\frac{1}{\rho}\frac{\partial p}{\partial y}+\frac{\mu}{\rho}\left(\frac{\partial^2 v}{\partial x^2}+\frac{\partial^2 v}{\partial y^2}+\frac{\partial^2 v}{\partial z^2}\right) \tag{3}$$

$$u\frac{\partial w}{\partial x}+v\frac{\partial w}{\partial y}+w\frac{\partial w}{\partial z}=-\frac{1}{\rho}\frac{\partial p}{\partial z}+\frac{\mu}{\rho}\left(\frac{\partial^2 w}{\partial x^2}+\frac{\partial^2 w}{\partial y^2}+\frac{\partial^2 w}{\partial z^2}\right) \tag{4}$$

where, p in Pa is pressure, ρ in kg/m^3 is density, and μ in Pa·s is viscosity.

The energy equations, in the fluid region:

$$\rho C_P\left(u\frac{\partial T}{\partial x}+v\frac{\partial T}{\partial y}+w\frac{\partial T}{\partial z}\right)=k_f\left(\frac{\partial^2 T}{\partial x^2}+\frac{\partial^2 T}{\partial y^2}+\frac{\partial^2 T}{\partial z^2}\right) \tag{5}$$

where, C_P, k_f and T are the specific heat of fluid, thermal conductivity, and fluid local temperature, respectively.

At the inlet, the Reynolds number is described as [51, 52]:

$$Re_{in}=\frac{\rho u_{in} D_h}{\mu} \tag{6}$$

where, D_h is the hydraulic diameter of the cross-sectional area at the inlet.

At steady state, the average convection heat transfer coefficient $\bar{h}$ on the bottom wall surface may be computed using [52]:

$$\bar{h}=\frac{q}{A_s(T_w-T_b)} \tag{7}$$

In the above equation, q is the heat flux, A_s represents the surface area, whereas T_s and T_b represent the average wall surface and bulk fluid temperatures, respectively.

The average Nusselt number is calculated based on the preceding equation [53, 54]:

$$\overline{Nu}=\frac{\bar{h}D_h}{k_f} \tag{8}$$

The friction factor (f) is depicted as follows [55]:

$$f=\Delta P\frac{D_h}{L}\frac{2}{\rho u_{in}} \tag{9}$$

where, ΔP is the pressure drop equals ($P_{out}-P_{in}$) and L represents channel length.

The performance evaluation criterion (PEC) utilized in this study may be stated as follows [52, 56]:

$$PEC=\frac{(\overline{Nu}_{,F}/\overline{Nu}_{,S})}{(f_{,F}/f_{,S})^{1/3}} \tag{10}$$

2.3 Boundary conditions

Silicon was selected as the solid walls of the microchannels, and water was the working fluid domain for this investigation. Table 3 shows the thermophysical characteristics of the materials at 300 K, which were taken to be temperature-independent. A working fluid inlet temperature of 300 K was established. A steady 800 KW/m^2 heat flux was used to heat the bottom wall. With no-slip velocity circumstances, it is assumed that the top walls and the side walls' outer surfaces are adiabatic. For the microchannel heat sink's inlet and outlet, the velocity inlet and pressure outlet boundary conditions are used, respectively. This study uses a Reynolds number that ranges from 100 to 500.

Table 3. Thermophysical properties for water and silicon are utilized in the current investigation

Materials	ρ (kg/m^3)	C_p (J/kg·K)	k (W/m·K)	μ (kg/m·s)
Water	998.2	4182	0.6103	0.001003
Silicon	2330	710	148	-

2.4 Numerical work

The Numerical calculation is conducted based on the commercial software ANSYS FLUENT 2020R1, based on the finite volume method (FVM) [57]. A pressure-based solver is adopted. The coupled pressure-velocity field was decoupled using the coupled algorithm, which allows for faster convergence. The gradient calculation uses a Least Squares Cell-Based scheme. The expression of diffusion in the momentum and energy equations was approximated by a second-order upwind. The calculation is considered to be converged when the iteration residual is less than 10^{-7} for the continuity, momentum, and energy equations.

3. GEOMETRY MESHING AND GRID INDEPENDENT TEST (GIT)

A suitably fine computational mesh is crucial, and this was the focus of efforts. All cases of MCHS were designed using ANSYS Design Modular. The geometry was divided into 108 bodies to get a suitable mesh (as shown in Figure 3(a) and 3(b)) and then defined as a fluid domain and a solid domain and thermally coupled together. The faces of the solid and fluid domains are named as inlet, outlet, insulated walls, symmetry walls, and heated wall. After that, export the geometric file to ANSYS meshing. Multi-zone method was selected for geometry in ANSYS meshing, which automatically generates a pure hexahedral mesh where possible. The GIT was performed for (MCHS-S) and (MCHS-C) before the simulation was carried out for the highest Reynolds number (Re = 500) while the node number is varied from 1.1 × 10^6 to 10.7 × 10^6. Since the increase in cell number after 6.75 × 10^6 for (MCHS-C) led to less than 0.3% of Nu, and f, and for (MCHS-S) led to less than 0.02%, thus, the cell number 6.75 ×10^6 is considered as mesh independence for (MCHS-C) and (MCHS-S) as shown in Figure 4.

Also, Figures 3(b) and 3(c) illustrate the intensity of the pure hexahedral mesh for both fluid and solid domains of the selected MCHS-C. The skewness, aspect ratio and orthogonal quality of mesh are also tested and it is found that the skewness, aspect ratio and orthogonal quality of MCHS-C are equal to 0.001, 31.5, and 0.99, respectively.

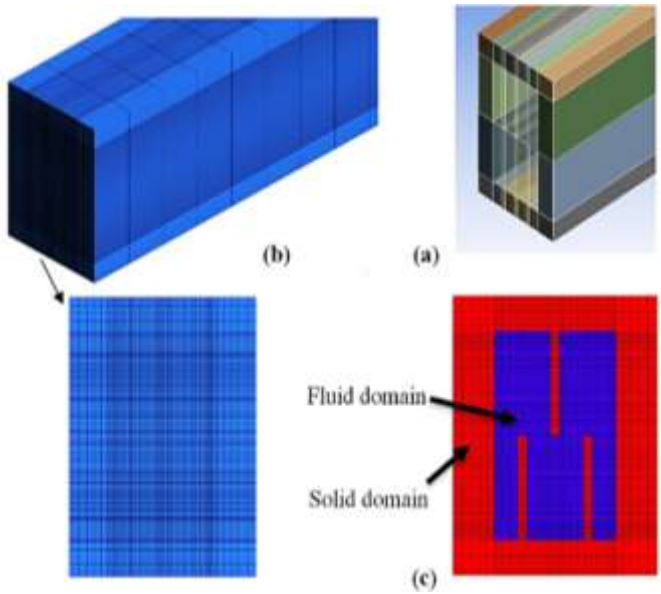

Figure 3. Display the meshing of geometry: (a) Division of geometry, (b) intensity of mesh, and (c) solid and fluid domain of MCHS-C

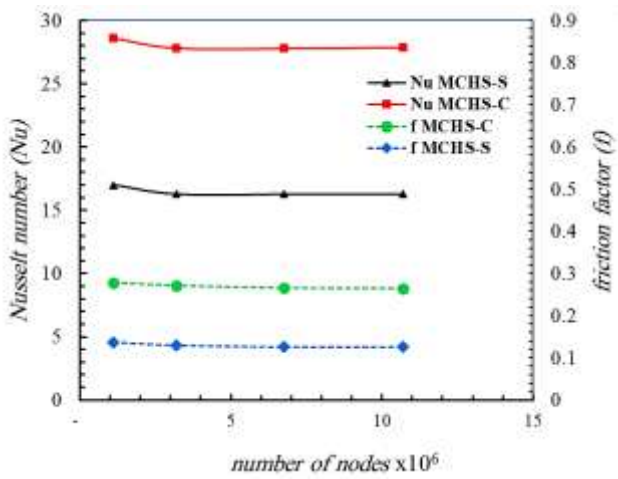

Figure 4. Nusselt number and friction factor versus number of nodes for MCHS-S and MCHS-C cases GIT

By plotting the Nusselt coefficient (Nu) and friction coefficient (f) against the number of nodes, Figure 4 shows the grid independent test (GIT) for the MCHS-S (baseline option) and MCHS-C (Case C with five fins). The findings indicate that Nu and f changes are negligible beyond 6.75 × 10^6 nodes, with variations of less than 0.3% for MCHS-C and 0.02% for MCHS-S. This shows that the mesh has enough detail to give accurate numerical results. The results show that the chosen grid size is both accurate and consistent, and it also costs less to compute. This mesh is a good balance between accuracy and usefulness for the purpose of studying how heat and fluid flow behave.

4. INITIAL VALIDATION INVESTIGATION

To verify the accuracy of the numerical CFD, a comparison was made with a numerical analysis of a channel featuring a single bifurcation plate along the centerline, following the

downstream path to the channel's outflow [58]. Figure 5 shows a comparison of wall temperature and channel length with the results of the current study's CFD. The results were rather consistent. Figure 6 shows how pressure drop affects channel length, and there is a strong agreement between the two studies, which shows that the data is real and correct.

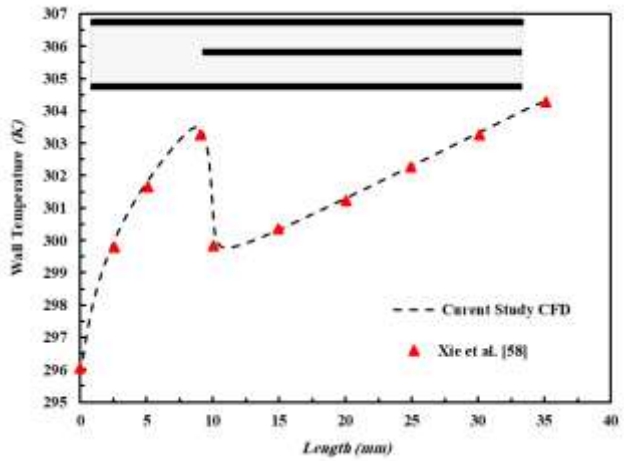

Figure 5. Validation of numerical results for wall Temperature with Xie et al. [58]

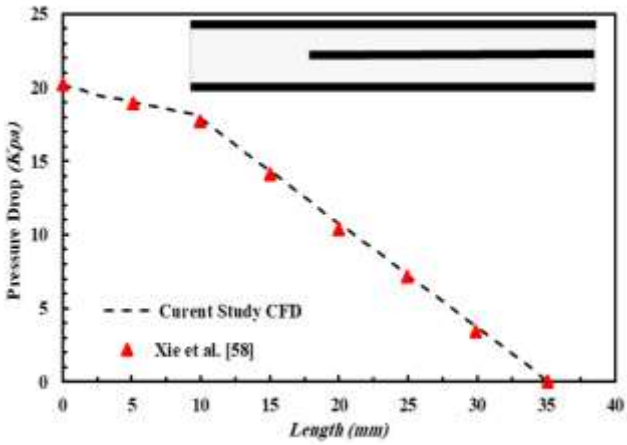

Figure 6. Validation of numerical results for pressure drop with Xie et al. [58]

Figures 5 and 6 back up the conclusions by comparing the study's numbers to those of earlier work by Xie et al. [58]. Figure 5, which shows how the temperature of the wall changes over the length of the channel, proves that the thermal equation is correct. It shows a high level of agreement with both the work of Xie et al. [58] and the current study. Figure 6 compares how the pressure drop changes over the length of the channel, which further proves that the simulation is accurate. The accuracy of the numerical approach is ensured by the constant trends shown in both figures. The accuracy of the study is confirmed by these validations, which offer a strong basis for examining how various fin configurations affect both the hydraulic and thermal characteristics of microchannel heat sinks.

5. RESULTS AND DISCUSSIONS

This section presents and discusses the effect of different types of fins with variable configurations (Cases A, B, and C), comparing them with the reference case (Case S) within the microchannel on the velocity and temperature contours at Re = 500.

The velocity contours for the micro-channel with variable configurations of fins and compared with the base topic (Case S), are presented in Figures 7 and 8. For (Case S), the flow is usually uniform as the fluid enters the micro-channel at a cold temperature. The velocity is highest at the center and decreases near the walls due to the effect of the boundary layer that begins forming at the micro-channel's inner surface. A boundary layer develops along the walls when the fluid moves through the micro-channel, which causes a change in the velocity distribution. A boundary layer develops along the walls when the fluid moves through the micro-channel, which causes a change in the velocity distribution. It is observed that the velocity reaches a steady state after the center of the microchannel, indicating the development of a full flow. For cases A and B, in the beginning, middle and end of the micro-channels, fins are clearly visible in the cross-section, designed to have a specific effect on the flow. It is noticed that the flow here is symmetrical and the highest velocity is found in the center and end of the micro-channel for cases A and B, respectively, depending upon the fins location. All fins change the velocity distribution, which interferes with the flow and causes velocity increases in the upper areas close to the fin and decreases in the lower areas. Furthermore, the fin leads to the splitting of the flow and increases the contact areas between the fluid and the surface, which improves the fluid mixing and heat transfer enhancement.

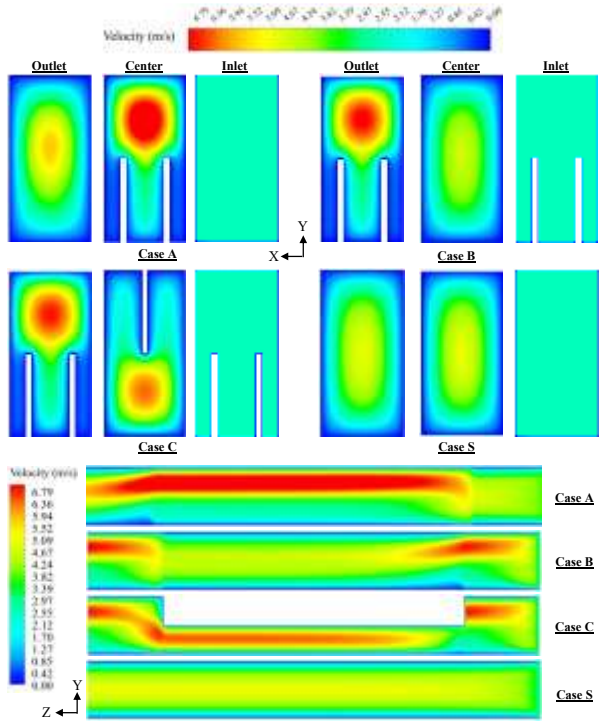

Figure 7. Velocity contours for variable configuration fins (Cases A, B, C, and S) at side and front views

Whereas, for Case C, the addition of a fin on the upper surface increases the velocity contour inside the microchannel. As stated earlier, with the presence of the fin, the cross-sectional area decreases at the middle portion of the micro-channel, which shows an increment in the flow velocity beneath the central fin near the heated surface. This local increase in velocity increases mixing and enhances the heat

transfer by increasing convective effects in the region. Case C thus has better thermal performance because of better mixing and enhanced convection heat transfer compared to cases without fins or with different configurations of fins.

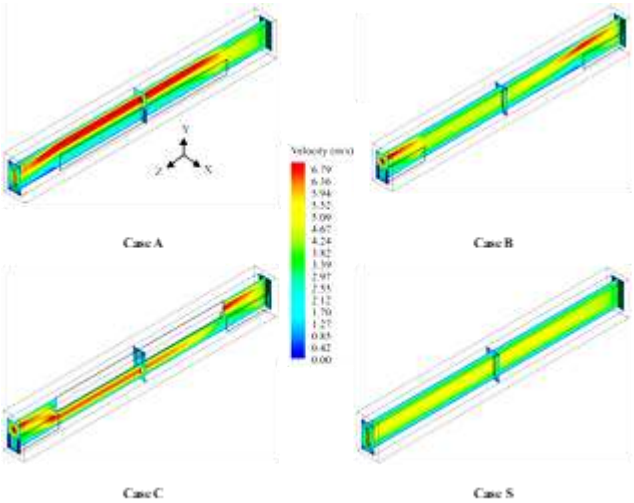

Figure 8. Velocity contours for varying configurations of fins (Cases A, B, C, and S) at 3D modelling views

Temperature contours for the micro-channel with different fin configurations (compared to the base case S) at Re = 500 are shown in Figure 9. For Case S, the temperature distribution shows a gradual decrease in temperature along the channel when the heat is transferred from the heated wall (at the inlet) to the fluid. However, the temperature difference between the fluid near the walls and the fluid in the middle of the channel remains large due to poor mixing. It is observed that the absence of fins results in a uniform (laminar) flow with minimal turbulence and mixing. Therefore, the heat transfer efficiency is low because the cold fluid in the center of the channel does not interact effectively with the heated wall. For the A and B cases, it is found that the presence of fins creates turbulence within the flow, which leads to improved fluid mixing. The thermal distribution shows a lower gradient compared to Case S, which means improved heat transfer. The thermal contours show that the fluid exits at a higher temperature compared to Case S, which means better thermal performance. For Case C, the fins show a greater improvement in mixing compared to the previous cases, as the thermal distribution appears more uniform along the channel. This is because the fin design in this case causes more efficient turbulence compared to the other cases. The results show that the temperature gradient on the hot wall is lower than in the previous two cases, indicating more enhancement of thermal transfer. The flow exiting the microchannel is at a higher temperature, proving that the thermal performance is better in this case.

Figure 10 presents the variation of the average Nusselt number with Reynolds number for different types of fin configurations in a microchannel heat sink (MCHS), which are compared with the baseline case without fins (MCHS-S). It is found that the average Nusselt number increased with increasing Reynolds number for all configurations due to the decreased thermal boundary layer thickness at the heated wall and the increased heat transfer rate at high flow [59]. It is discovered that adding fins in different arrangements significantly influences the mean Nusselt number. Furthermore, it is observed that the highest Nusselt number values were obtained at the MCHS-C compared to the other designs for all Reynolds ranges. This is due to the upper fin improving the mixing flow and enhancing heat transfer. Results indicated that the micro-channel heat sink Type A achieves a higher heat transfer than MCHS-B and MCHS-S due to the effect of fin arrangement. The outcomes indicated that using fins improved the mean Nusselt number by 66, 36, and 31% for designs Case C, A, and B, respectively, compared to the base case at Re = 500.

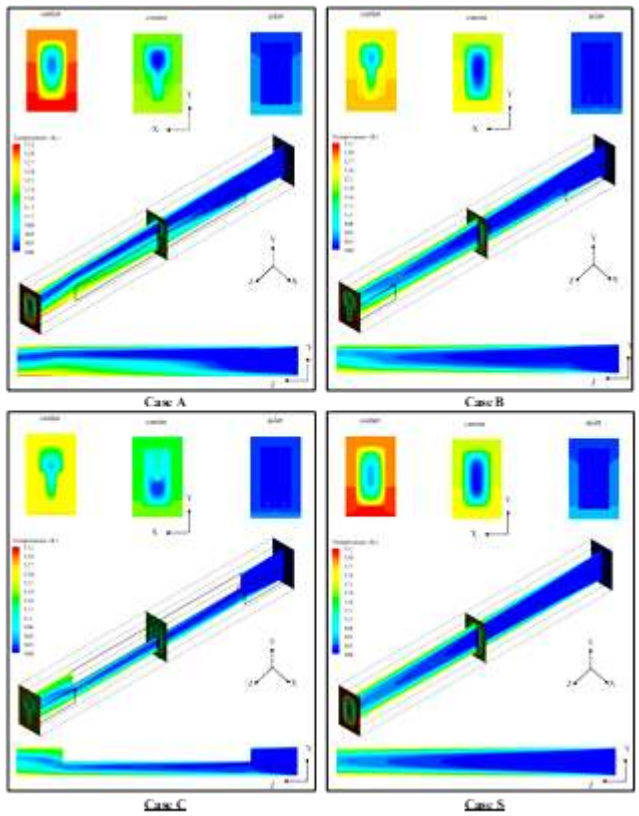

Figure 9. Temperature contours for varying configurations of fins (Cases A, B, C, and S) at the side, front 3D, and modelling views

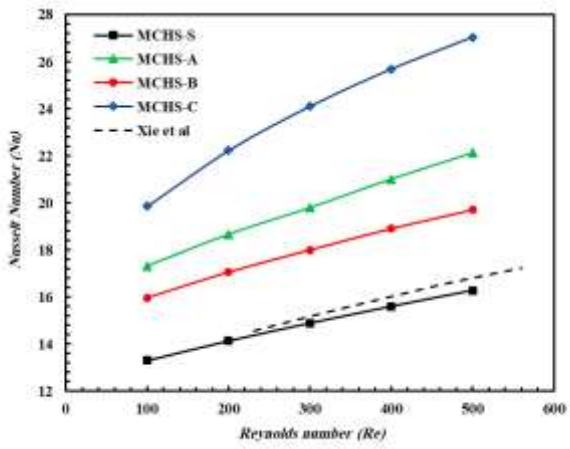

Figure 10. Effects of varying configurations of fins (MCHS A, B, C, and S) on the average Nusselt number

Figure 11 presents the variation of the friction factor with Reynolds number for various kinds of fin configurations in the MCHS. It is observed that as the Reynolds number increases, the friction factor reduces for all configurations. Moreover, the baseline case (MCHS-S) has a lower friction factor due to the

absence of obstruction to the fluid flow. With the addition of fins, it was found that case MCHS-C provided the highest flow losses, followed by cases (MCHS-A and MCHS-B) due to the flow obstruction and the recirculation that occurs downstream of the fin.

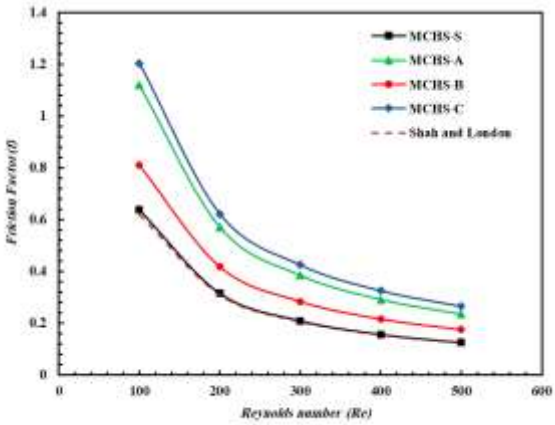

Figure 11. Effects of varying configurations of fins (MCHS A, B, C, and S) on the friction factor

Figure 12 shows the relation between wall temperature and Reynolds number for different types of fin designs in the MCHS. It is found that the wall temperature decreases with increased Reynolds number for all designs due to the high flow velocity. Furthermore, MCHS-C provided the lowest wall temperatures across the entire range of Reynolds numbers, followed by cases (MCHS-A and MCHS-B). Correspondingly, the reference case (MCHS-S) achieves a high wall temperature due to poor flow mixing and limited heat transfer efficiency.

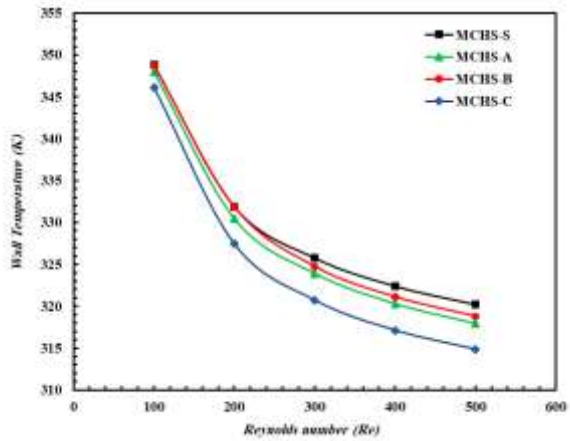

Figure 12. Effects of varying configurations of fins (MCHS A, B, C, and S) on the wall temperature

The relation between the Reynolds range and the PEC for particular fin shapes used in microchannel coolers (MCHS) is shown in Figure 13. It was found that all values of the PEC are more than unity in all cases. From the results, it is clear that MCHS-C has the greatest PEC (about 1.3) at Re = 500 compared to other configurations. This illustrates how well the MCHS-C gadget performs in striking a balance between a heat transfer enhancement and fewer friction losses. In contrast to the MCHS-C, the PEC values for the MCHS-A and MCHS-B configurations are still near cohesion with minimal fluctuation inside the improved Reynolds quantity, suggesting that they have less of an effect on performance.

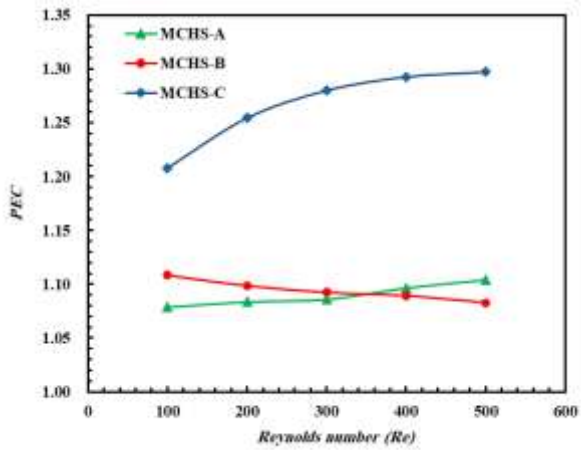

Figure 13. Effects of variable configurations of fins (MCHS A, B, C, and S) on the PEC

6. CHALLENGES

To create effective thermal management systems, it is necessary to overcome a number of obstacles related to the construction and optimization of microchannel thermal sinks (MCHS) with different fin designs. Computerized modeling, experimental verification, material selection, flow dynamics, and practical implementation are only a few of the several domains impacted by these obstacles. Detailed solutions to these problems in five separate areas are provided below:

6.1 Complexity of computational modeling

One of the main issues with studying very small heat exchangers is that it's hard to construct computer models that are realistic. You have to answer a number of hard math problems at once. These are some of the things that happen: How heat transfers, how energy is kept in balance, and how gases and liquids act. We used the FVM and ANSYS software to do this project. This method is known to take a lot of computer power, especially when you're working with shapes that are hard to interpret or places that need highly exact calculations. Figure 4 demonstrates that as you make the calculation areas smaller and smaller, the Nusselt number and the friction factor will also be smaller. That's an important first step: we need to make sure that the calculation grid we used didn't affect our results in any way. You can get to that point where the grid doesn't impact the result, but it still takes a lot of computing power, especially when you're working with tough heat exchanger designs like Case C.

6.2 Limitations of experimental validation

CFD models of fluid flow teach us a lot, but we still need to test them in the actual world to make sure they stay accurate. Figures 5 and 6 show that our investigation's results are in agreement with those of Xie et al. [58]. The computer's predictions may not match the actual results of the study. There may not be any set regulations controlling the system, materials may differ, and manufacturing processes may change. For example, having completely smooth surfaces could make it hard to make little channels of the right size. Reproducing an experiment under conditions as near as the ones predicted by the models is not always possible. Inadequate wall insulation and inconsistent water flow are two

of the many possible problems. New and better measuring instruments are necessary to close the gap between virtual and physical environments.

6.3 Choosing materials and managing heat

A micro channel heat sink's efficiency is highly dependent on the materials used to build it. Silicon, with its remarkable microfabrication capabilities and high heat conductivity, was selected as the experimental material. Because of its high price and structural instability, silicon isn't great for a lot of commercial uses. Copper and aluminum are superior to other materials when it comes to heat permeability, corrosion resistance, and compatibility with coolants. Additionally, over time, fouling or degradation may result from the coolant's interaction with the channel walls, which would lower long-term performance. It's still quite difficult to create long-lasting, reasonably priced materials that resist corrosion and wear while retaining good heat conductivity. developments in nanotechnology.

6.4 Trade-offs between flow dynamics versus pressure drop

Innovative fin designs that improve heat transfer frequently result in higher flow resistance and pressure drop. All fin arrangements (Cases A, B, and C) showed higher friction factors than the baseline example (example S), as shown in Figure 11. Fins increase surface area and turbulence, which enhances heat transmission, but they also disturb the flow field, creating recirculation zones and requiring more pumping force. Finding the sweet spot between permissible pressure drop and heat transfer enhancement is a major problem in MCHS design. This trade-off becomes more apparent at higher Reynolds numbers, when the benefits of better mixing have to be weighed against the disadvantages of increasing flow losses.

6.5 Scalability and real-world application

Finally, there are a lot of challenges when trying to turn ideas for cooling systems into practical ones. Microchannel heat sinks are commonly used in small electronic devices where there is little room for design freedom due to manufacturing tolerances or space constraints. Additional complications arise when these systems are scaled up for larger applications, like photovoltaic cooling or industrial heat exchangers. For instance, as the entire system size increases, it becomes more challenging to maintain consistent flow distribution over several parallel channels. Hotspots and decreased performance might result from uneven flow. Additionally, careful investigation into system-level interactions is necessary when integrating MCHS with current cooling infrastructures, such as pumping and reservoirs. In order to provide scalable and dependable solutions, addressing these issues requires interdisciplinary approaches that combine knowledge of thermal engineering, substance science, and manufacturing technology.

In conclusion, even though microchannel cooling systems with fin topologies that are tuned have a great deal of promise to improve thermal performance, their widespread adoption depends on resolving the issues outlined above. Researchers may create the foundation for next-generation cooling techniques that satisfy the needs of contemporary electronics and beyond by developing computational tools, refining experimental procedures, investigating new materials, maximizing flow dynamics, and resolving scalability concerns.

7. CONCLUSIONS

In order to optimize cooling systems for contemporary electronic devices, this study offers a thorough numerical analysis of the hydraulic and thermal efficiency of microchannel cooling systems (MCHS) with different fin designs. The study compares three different fin configurations (Cases A, B, and C) to a baseline example with no fins (Case S) using the finite volume technique with ANSYS software over a range of Reynolds numbers from 100 to 500. The findings highlight how important fin design is for increasing heat exchange rates while balancing related trade-offs like friction losses and pressure drop.

The results show that adding fins greatly enhances heat transfer performance; for Re = 500, Case C showed the largest improvement, at 66%, followed by Case A (36%) and Case B (31%). Increased turbulence, improved mixing, and a larger contact area between the fluid and the surface that is heated, made possible by the fins, are the reasons for this improvement. Additionally, in every case, an average Nusselt number rises with Reynolds number, emphasizing the advantages of greater flow rates in enhancing convective heat transfer and decreasing the thickness of the thermal boundary layer. On the other hand, when the Reynolds number rises, the average wall temperature and friction factor fall, highlighting the significance of striking a balance between thermal performance and flow efficiency.

With a thermal-hydraulic performance coefficient (PEC) of roughly 1.3 at Re = 500, Case C is the most effective design. The highest (PEC) for Cases (A, B) is around 1.10 at Re = 100 and 1.11 at Re = 500, respectively. This product works better because its revolutionary design keeps the temperature steady along the channel and makes convection stronger. These experiments show how innovative fin designs can assist in meeting the increased demand for small, very effective cooling systems in microelectronics.

The research emphasizes the importance of using computer simulations in the creation of tiny heating elements. However, it also points out that achieving trustworthy and scalable results requires tackling several key hurdles: making sure the simulation's accuracy isn't affected by the fineness of the mesh, confirming the model's accuracy through experiments, and carefully choosing the right materials. Overcoming these challenges will allow for improvements in thermal management, leading to the creation of better and more energy-saving cooling technologies. The work highlights the revolutionary potential of improved fin configurations in fulfilling the thermal needs of next-generation electronics by connecting theoretical analysis with real-world applications.

8. FUTURE WORK

The following determinants can be suggested for future work:

- Improving the heat transfer of microchannels by adding fins of different shapes under the influence of turbulent flow.

- Numerical and experimental study of improving the thermal performance factor of three-dimensional microchannels using nanofluids.

REFERENCES

[1] Al-Baghdadi, M.A.R.S., Noor, Z.M.H., Zeiny, A., Burns, A., Wen, D. (2020). CFD analysis of a nanofluid-based microchannel heat sink. Thermal Science and Engineering Progress, 20: 100685. http://doi.org/10.1016/j.tsep.2020.100685

[2] Bickley, H.D. (1983). Cooling of electronic equipment. Electronics and Power, 29(5): 386. https://doi.org/10.1049/ep.1983.0178

[3] Abo-Zahhad, E.M., Ookawara, S., Radwan, A., El-Shazly, A.H., ElKady, M.F. (2018). Thermal and structure analyses of high concentrator solar cell under confined jet impingement cooling. Energy Conversion and Management, 176: 39-54. https://doi.org/10.1016/j.enconman.2018.09.005

[4] Solbrekken, G.L., Yazawa, K., Bar-Cohen, A. (2004). Thermal management of portable electronic equipment using thermoelectric energy conversion. In the Ninth Intersociety Conference on Thermal and Thermomechanical Phenomena in Electronic Systems (IEEE Cat. No.04CH37543), Las Vegas, NV, USA, pp. 276-283. https://doi.org/10.1109/ITHERM.2004.1319185

[5] Alhattab, H.A., Sadiq Al-Baghdadi, M.A.R., Hashim, R.S., Ali, A.H. (2016). Design of micro heat sink for power transistor by using CFD. In 2016 Al-Sadeq International Conference on Multidisciplinary in IT and Communication Science and Applications (AIC-MITCSA), Baghdad, Iraq, pp. 1-5. http://doi.org/10.1109/AIC-MITCSA.2016.7759948

[6] Zeng, L., Deng, D., Zhong, N., Zheng, G. (2021). Thermal and flow performance in microchannel heat sink with open-ring pin fins. International Journal of Mechanical Sciences, 200: 106445. http://doi.org/10.1016/j.ijmecsci.2021.106445

[7] Zhu, Q., Xia, H., Chen, J., Zhang, X., Chang, K., Zhang, H., Jin, Y. (2021). Fluid flow and heat transfer characteristics of microchannel heat sinks with different groove shapes. International Journal of Thermal Sciences, 161: 106721. https://doi.org/10.1016/j.ijthermalsci.2020.106721

[8] Zhu, Q., Jin, Y., Chen, J., Su, R., Zhu, F., Li, H., Xia, H. (2021). Computational study of rib shape and configuration for heat transfer and fluid flow characteristics of microchannel heat sinks with fan-shaped cavities. Applied Thermal Engineering, 195: 117171. https://doi.org/10.1016/j.applthermaleng.2021.117171

[9] Copeland, D., Behnia, M., Nakayama, W. (1997). Manifold microchannel heat sinks: Isothermal analysis. IEEE Transactions on Components, Packaging, and Manufacturing Technology: Part A, 20(2): 96-102. https://doi.org/10.1109/95.588554

[10] Chu, Y.M., Farooq, U., Mishra, N.K., Ahmad, Z., Zulfiqar, F., Yasmin, S., Khan, S.A. (2023). CFD analysis of hybrid nanofluid-based microchannel heat sink for electronic chips cooling: Applications in nano-energy thermal devices. Case Studies in Thermal Engineering, 44: 102818. http://doi.org/10.1016/j.csite.2023.102818

[11] Liao, S.M., Zhao, T.S. (2002). An experimental investigation of convection heat transfer to supercritical carbon dioxide in miniature tubes. International Journal of Heat and Mass Transfer, 45(25): 5025-5034. https://doi.org/10.1016/S0017-9310(02)00206-5

[12] Ashjaee, M., Goharkhah, M., Khadem, L.A., Ahmadi, R. (2015). Effect of magnetic field on the forced convection heat transfer and pressure drop of a magnetic nanofluid in a miniature heat sink. Heat and Mass Transfer, 51(7): 953-964, http://doi.org/10.1007/s00231-014-1467-1

[13] Chai, L., Xia, G., Wang, L., Zhou, M., Cui, Z. (2013). Heat transfer enhancement in microchannel heat sinks with periodic expansion – constriction cross-sections. International Journal of Heat and Mass Transfer, 62: 741-751. https://doi.org/10.1016/j.ijheatmasstransfer.2013.03.045

[14] Xie, G., Chen, Z., Sunden, B., Zhang, W. (2013). Numerical analysis of flow and thermal performance of liquid-cooling microchannel heat sinks with bifurcation. Numerical Heat Transfer, Part A: Applications, 64(11): 37-41. https://doi.org/10.1080/10407782.2013.807689

[15] Xie, G., Li, S., Sunden, B., Zhang, W., Li, H. (2014). A numerical study of the thermal performance of microchannel heat sinks with multiple length bifurcation in laminar liquid flow. Numerical Heat Transfer, Part A: Applications, 65(2): 107-126. https://doi.org/10.1080/10407782.2013.826084

[16] Chai, L., Dong, G., Sheng, H. (2016). Parametric study on thermal and hydraulic characteristics of laminar flow in microchannel heat sink with fan-shaped ribs on sidewalls – Part 3: Performance evaluation. International Journal of Heat and Mass Transfer, 97: 1091-1101. https://doi.org/10.1016/j.ijheatmasstransfer.2016.02.075

[17] Chai, L., Xia, G.D., Wang, H.S. (2016). Parametric study on thermal and hydraulic characteristics of laminar flow in microchannel heat sink with fan-shaped ribs on sidewalls - Part 1: Heat transfer. International Journal of Heat and Mass Transfer, 97: 1081-1090. https://doi.org/10.1016/j.ijheatmasstransfer.2016.02.077

[18] Chai, L., Xia, G.D., Wang, H.S. (2016). Parametric study on thermal and hydraulic characteristics of laminar flow in microchannel heat sink with fan-shaped ribs on sidewalls - Part 2: Pressure drop. International Journal of Heat and Mass Transfer, 97: 1081-1090. https://doi.org/10.1016/j.ijheatmasstransfer.2016.02.076

[19] Lu, G., Zhao, J., Lin L., Wang, X., Yan, W. (2017). A new scheme for reducing pressure drop and thermal resistance simultaneously in microchannel heat sinks with wavy porous fins. International Journal of Heat and Mass Transfer, 111: 1071-1078. https://doi.org/10.1016/j.ijheatmasstransfer.2017.04.086

[20] Wang, R., Wang, J., Lijin, B., Zhu, Z. (2018). Parameterization investigation on the microchannel heat sink with slant rectangular ribs by numerical simulation. Applied Thermal Engineering, 133: 428-438. http://doi.org/10.1016/j.applthermaleng.2018.01.021

[21] Shen, H., Wang, C., Xie, G. (2018). A parametric study on thermal performance of microchannel heat sinks with internally vertical bifurcations in laminar liquid flow. International Journal of Heat and Mass Transfer, 117: 487-497. https://doi.org/10.1016/j.ijheatmasstransfer.2017.10.025

[22] Li, P., Luo, Y., Zhang, D., Xie, Y. (2018). Flow and heat transfer characteristics and optimization study on the water-cooled microchannel heat sinks with dimple and pin fin. International Journal of Heat and Mass Transfer, 119: 152-162. https://doi.org/10.1016/j.ijheatmasstransfer.2017.11.112
[23] Lee, S., Choi, S.U.S., Li, S., Eastman, J.A. (1999). Measuring thermal conductivity of fluids containing oxide nanoparticles. Journal of Heat and Mass Transfer, 121(2): 280-289. https://doi.org/10.1115/1.2825978
[24] Choi, S.U.S., Eastman, J.A. (1995). Enhancing thermal conductivity of fluids with nanoparticles. In Proceedings of the ASME 1995 International Mechanical Engineering Congress and Exposition. Developments and Applications of Non-Newtonian Flows, San Francisco, California, USA, pp. 99-105. https://doi.org/10.1115/IMECE1995-0926
[25] Wen, D., Lin, G., Vafaei, S., Zhang, K. (2009). Review of nanofluids for heat transfer applications. Particuology, 7(2): 141-150. https://doi.org/10.1016/j.partic.2009.01.007
[26] Buongiorno, J., Venerus, D.C., Prabhat, N., McKrell, T., et al. (2009). A benchmark study on the thermal conductivity of nanofluids. Journal of Applied Physics, 106(9): 094312. https://doi.org/10.1063/1.3245330
[27] Kareem, M.K., Abed, W.M., Dawood, H.K. (2020). Numerical simulation of hydrothermal behavior in a concentric curved annular tube. Heat Transfer, 49(5): 2494-2520. https://doi.org/10.1002/htj.21732
[28] Sadiq Al-Baghdadi, M.A.R. (2010). A CFD analysis of transport phenomena and electrochemical reactions in a tubular-shaped ambient air-breathing PEM micro fuel cell. HKIE Transactions, 17(2): 1-8. https://doi.org/10.1080/1023697X.2010.10668189
[29] Sadiq Al-Baghdadi, M.A.R. (2009). A CFD study of hygro-thermal stresses distribution in PEM fuel cell during regular cell operation. Renewable Energy, 34(3): 674-682. https://doi.org/10.1016/j.renene.2008.05.023
[30] Sadiq Al-Baghdadi, M.A.R. (2009). Prediction of deformation and hygro-thermal stresses distribution in ambient air-breathing PEM fuel cells using three-dimensional CFD model. Recent Patents on Mechanical Engineering, 2(1): 26-39. http://doi.org/10.2174/2212797610902010026
[31] Qu, W., Mudawar, I. (2002). Experimental and numerical study of pressure drop and heat transfer in a single-phase micro-channel heat sink. International Journal of Heat and Mass Transfer, 45(12): 2549e2565. https://doi.org/10.1016/S0017-9310(01)00337-4
[32] Xie, X.L., Tao, W.Q., He, Y.L. (2007). Numerical study of turbulent heat transfer and pressure drop characteristics in a water-cooled minichannel heat sink. Journal of Electronic Packaging, 129(3): 247-255. https://doi.org/10.1115/1.2753887
[33] Xie, X.L., Liu, Z.J., He, Y.L., Tao, W.Q. (2009). Numerical study of laminar heat transfer and pressure drop characteristics in a water-cooled minichannel heat sink. Applied Thermal Engineering, 29: 64-74. https://doi.org/10.1016/j.applthermaleng.2008.02.002
[34] Sui, Y., Teo, C.J., Lee, P.S., Chew, Y.T., Shu, C. (2010). Fluid flow and heat transfer in wavy microchannels. International Journal of Heat and Mass Transfer, 53: 2760-2772. https://doi.org/10.1016/j.ijheatmasstransfer.2010.02.022
[35] Xie, G.N., Liu, J., Zhang, W.H., Sunden, B. (2012). Analysis of flow and thermal performance of a water-cooled transversal wavy microchannel heat sink for chip cooling. Journal of Electronic Packaging, 134(4): 041010. https://doi.org/10.1115/1.4023035
[36] Xie, G.N., Liu, J., Liu, Y.Q., Sunden, B., Zhang, W.H. (2013). Comparative study of thermal performance of longitudinal and transversal wavy microchannel heat sinks for electronic cooling. Journal of Electronic Packaging, 135(2): 021008. https://doi.org/10.1115/1.4023530
[37] Zhang, J.R., Jaluria, Y., Zhang, T.T., Jia, L. (2012). Combined experimental and numerical study for multiple microchannel heat transfer system. Numerical Heat Transfer, Part B: Fundamentals, 64(4): 293-305. https://doi.org/10.1080/10407790.2013.791781
[38] Zhang, J.R., Lin, P.T., Jaluria, Y. (2012). Designs of multiple microchannel heat transfer systems. In Proceedings of the ASME 2011 International Mechanical Engineering Congress and Exposition, Volume 11: Nano and Micro Materials, Devices and Systems; Microsystems Integration, Denver, Colorado, USA, pp. 875-887. https://doi.org/10.1115/IMECE2011-62539
[39] Wang, X.Q., Mujumdar, A.S., Yap, C. (2006). Thermal characteristics of tree-shaped microchannel nets for cooling of a rectangular heat sink. International Journal of Thermal Sciences, 45(11): 1103-1112. https://doi.org/10.1016/j.ijthermalsci.2006.01.010
[40] Wang, X.Q., Xu, P., Mujumdar, A.S., Yap, C. (2010). Flow and thermal characteristics of offset branching network. International Journal of Thermal Sciences, 49(2): 272-280. https://doi.org/10.1016/j.ijthermalsci.2009.07.019
[41] Gilmore, N., Timchenko, V., Menictas, C. (2018). Microchannel cooling of concentrator photovoltaics: A review. Renewable and Sustainable Energy Reviews, 90: 1041-1059. https://doi.org/10.1016/j.rser.2018.04.010
[42] Naqiuddin, N.H., Saw, L.H., Yew, M.C., Yusof, F., Ng, T.C. (2018). Overview of micro-channel design for high heat flux application. Renewable and Sustainable Energy Reviews, 82: 901-914. https://doi.org/10.1016/j.rser.2017.09.110
[43] Di Capua, H.M., Escobar, R., Diaz, A.J., Guzman, A.M. (2018). Enhancement of the cooling capability of a high concentration photovoltaic system using microchannels with forward triangular ribs on sidewalls. Applied Energy, 226: 160-180. https://doi.org/10.1016/j.apenergy.2018.05.052
[44] Alfellag, M.A., Ahmed, H.E., Kherbeet, A.S. (2020). Numerical simulation of hydrothermal performance of minichannel heat sink using inclined slotted plate-fins and triangular pins. Applied Thermal Engineering, 164: 114509. https://doi.org/10.1016/j.applthermaleng.2019.114509
[45] Ali, N., Haque, I., Alam, T., Siddiqui, T.U., Ansari, M.A., Yadav, J., Srivastava, S., Cuce, E., Ashraf, I., Dobrotă, D. (2025). Numerical investigation on heat transfer and flow mechanism in microchannel heat sink having V shape ribs. Case Studies in Thermal Engineering, 65: 105684. https://doi.org/10.1016/j.csite.2024.105684
[46] Okab, A.K., Hasan, H.M., Hamzah, M., Egab, K., Al-Manea, A., Yusaf, T. (2022). Analysis of heat transfer and fluid flow in a microchannel heat sink with sidewall

dimples and fillet profile. International Journal of Thermofluids, 15: 100192. https://doi.org/10.1016/j.ijft.2022.100192
[47] Ali, S., Alam, S., Khan, M.N. (2024). Effect of cylindrical ribs arrangement in the cavity region of the microchannel heatsink with a fan-shaped cavity. In Proceedings of the Institution of Mechanical Engineers, Part E: Journal of Process Mechanical Engineering. https://doi.org/10.1177/09544089241231481
[48] Li, C., Chen, W. (2024). Thermo-hydraulic analysis in double-layered microchannels with porous rib and phase change microcapsules slurry as coolant. International Communications in Heat and Mass Transfer, 155: 107489. https://doi.org/10.1016/j.icheatmasstransfer.2024.107489
[49] Li, B., Cui, Y., Li, G., Jiang, H. (2024). Numerical analysis on thermal-hydraulic performance of optimized microchannel heat sink with slant ribs and quatrefoil rib-elliptical groove complex structures. Applied Thermal Engineering, 240: 122165. https://doi.org/10.1016/j.applthermaleng.2023.122165
[50] Bejan, A. (2013). Convection Heat Transfer. Hoboken, NJ: John Wiley & Sons. http://doi.org/10.1002/9781118671627
[51] Thabit, S.M., Abed, W.M. (2023). Experimental and numerical convective heat transfer investigation in laminar rectangular-channel flow across V-shaped grooves. Journal of Enhanced Heat Transfer, 30(2): 35-67. http://doi.org/10.1615/JEnhHeatTransf.2022044000
[52] Bergman, T.L., Lavine, A.S., Incropera, F.P., DeWitt, D.P. (2011). Introduction to Heat Transfer. New York: John Wiley & Sons.
[53] Ahmed, M.A., Hatem, S.M., Alabdaly, I.K. (2024). Investigation of heat transfer enhancement and entropy increment in a U channel with V-shaped ribs for improved hydrothermal performance. International Journal of Heat & Technology, 42(2): 455-465. http://doi.org/10.18280/ijht.420211
[54] Ahmed, M.A., Alabdaly, I.K., Hatem, S.M., Hussein, M.M. (2024). Numerical investigation on heat transfer enhancement in serpentine mini-channel heat sink. International Journal of Heat and Technology, 42(1): 183-190. https://doi.org/10.18280/ijht.420119
[55] Dawood, H., Mohammed, H., Sidik, N.A.C., Munisamy, K. (2015). Numerical investigation on heat transfer and friction factor characteristics of laminar and turbulent flow in an elliptic annulus utilizing nanofluid. International Communications in Heat and Mass Transfer, 66: 148-157. https://doi.org/10.1016/j.icheatmasstransfer.2015.05.019
[56] Ahmed, M.A., Alabdaly, I.K., Hatema, S.M., Hussein, M.M. (2023). Numerical investigation of hydrothermal performance and entropy generation through backward facing step channel with oval rib. International Journal of Heat and Technology, 41(5): 1349-1357. https://doi.org/10.18280/ijht.410526
[57] ANSYS, Ansys Fluent Theory Guide, Ansys Inc., pp. 724–746, 2011.
[58] Xie, G., Zhang, F., Sundén, B., Zhang, W. (2014). Constructal design and thermal analysis of microchannel heat sinks with multistage bifurcations in single-phase liquid flow. Applied Thermal Engineering, 62(2): 791-802. https://doi.org/10.1016/j.applthermaleng.2013.10.042
[59] Alabdaly, I.K., Hatem, S.M., Ahmed, M.A., Abed, T.H., Al-Amir, Q.R. (2025). Numerical investigation of hydrothermal characteristics in backward-facing Step Channel with Obstacles. International Journal of Heat and Technology, 43(1): 309-318. https://doi.org/10.18280/ijht.430131

NOMENCLATURE

A_s	surface area, mm^2
C_P	specific heat, J/kg·K
CFD	computational fluid dynamics
D_h	hydraulic diameter, mm
F	friction factor
H	microchannel height, μm
H	heat transfer coefficients, W/m^2·K
$\bar{h}$	average heat transfer coefficients, W/m^2·K
K	thermal conductivity, W/m·K
L	microchannel length, μm
MCHS	micro-channel heat sink
MEMS	micro-electro-mechanical-systems
Nu	Nusselt number
PEC	performance evaluation criterion factor
P	pressure, Pa
Q	heat flux, W/m^2
Re	Reynolds number
T	temperature, K
T_s	average wall surface, K
T_b	bulk fluid temperatures, K
u, v, w	velocity components, m/s
x, y, z	3D cartesian coordinates, mm
W	microchannel width, μm

Greek symbols

Δp	pressure drop, pa
P	density, kg/m^3
μ	dynamic viscosity, N·s/m^2
б	surface tension, N/m

Subscripts

in	inlet
out	outlet